Eur. Phys. J. A **36**, 31–36 (2008)
DOI 10.1140/epja/i2007-10548-5

THE EUROPEAN
PHYSICAL JOURNAL A

Regular Article – Experimental Physics

Bremsstrahlung emission accompanying the α-decay of ^{214}Po

G. Giardina[1,a], G. Fazio[1], G. Mandaglio[1], M. Manganaro[1], C. Saccá[2], N.V. Eremin[3], A.A. Paskhalov[3], D.A. Smirnov[3], S.P. Maydanyuk[4], and V.S. Olkhovsky[4]

[1] Dipartimento di Fisica dell'Università di Messina, 98166 Messina, Italy
[2] Dipartimento di Scienze della Terra dell'Università di Messina, 98166 Messina, Italy
[3] Skobeltsin Institute of Nuclear Physics, Lomonosov Moscow State University, 119899 Moscow, Russia
[4] Institute for Nuclear Research, National Academy of Science of Ukraine, 03680 Kiev, Ukraine

Received: 14 November 2007 / Revised: 18 January 2008
Published online: 10 April 2008 –
Communicated by C. Signorini

Abstract. We analyze the bremsstrahlung emission obtained by the α-γ coincidence measurements to investigate on the α-decay dynamics of the ^{214}Po nucleus. We performed the experiment using a radioactive ^{226}Ra source leading, by α-decays, to the ^{214}Po nucleus, and the apparatus with the Si detector for α-particles, the NaI(Tl) detector able to collect photons with energies up to about 1 MeV. We compare the experimental data with the quantum-mechanical calculations and find a good agreement between theory and experiment for photon energies up to 765 keV. In the experimental data of the bremsstrahlung spectrum one can see the presence of slight oscillations.

PACS. 23.60.+e α decay – 23.20.-g Electromagnetic transitions – 27.80.+w $190 \leq A \leq 219$ – 27.90.+b $220 \leq A$

1 Introduction

In recent years many attempts have been made to study the nature of the bremsstrahlung emission in the α-decay of heavy nuclei. After the first theoretical description concerning the possibility of the photon emission with energy higher than 200 keV in the tunneling process during the α-decay of ^{210}Po [1], in our previous works we obtained the energy spectra of photons accompanying the α-decays of the ^{214}Po and ^{226}Ra, and ^{210}Po nuclei [2,3], respectively. Kasagi *et al.* [4,5] reported the results of the bremsstrahlung emission in the α-decay of the ^{210}Po and ^{244}Cm nuclei. In the energy spectrum of the bremsstrahlung radiation associated with the α-decay of ^{210}Po the authors [4, 5] observed the minimum in the range of E_γ energies of about 400 keV. The theoretical analysis of these data in the framework of different models [6–9] did not agree with the assumption of the destructive interference of the radiation amplitudes between the inside and the outside of the barrier [4,5]. In addition, the authors of ref. [10] found the negative interference effect of the bremsstrahlung emission amplitudes related to the motion of the α-particle in the sub-barrier region (also including the reflection component) and inside the barrier, even if the contribution of the inside-barrier radiation is always several times smaller than the outside-barrier one (at the left and right sides of the barrier). Other experimental results for ^{210}Po had been lately presented in the paper by Boie *et al.* [11] where the authors have not observed the minimum found by Kasagi *et al.* [4].

Therefore, the main problem to investigate the dynamics of the α-particle tunneling through the Coulomb barrier of the nucleus is how to obtain a better experimental statistics for high energies of photons (higher than some hundred keV). In the present paper we reconsider our old experimental results [2] and obtain new ones for the bremsstrahlung emission in the α-decay of ^{214}Po up to about $E_\gamma = 800$ keV.

2 Experiment

The experimental set-up was the same as described in our previous paper [2]. The radioactive ^{226}Ra source with an activity of about 10^4 α-particles/s was chosen. Along the decay chain of this nucleus, the α-particle leading to the ^{214}Po isotope was recorded. The diameter of the radioactive spot on the source surface was about 8 mm and the α-particles were detected with a silicon surface barrier detector with energy resolution of about 20 keV at the α-particle energy of 5.3 MeV. The α detector was 200 mm^2 in area and was placed at a distance of about 1 cm from the source. The time resolution of the α-γ coincidence technique was $\tau = 10$ ns.

[a] e-mail: giardina@nucleo.unime.it

To increase the statistics we changed, with respect to the previous experimental configuration [2], the photon detector and its distance from the radioactive source. The γ-rays were detected by the NaI(Tl) detector with a diameter of 3 cm and a thickness of 3 cm, and the distance between the source and the γ detector was about 1.6 cm. The angles between the two detectors and the normal axis to the surface of the source were 45°. So the total angle between the α and γ detectors was about 90°. This angle value was chosen to increase the yield of the $E1$ dipole bremsstrahlung photons and to reduce the influence of γ-rays from the $E2$ quadrupole transitions of the excited states of daughter nuclei.

The absolute values of the NaI(Tl) detector efficiency for photon energies from 60 keV up to 1 MeV were determined by measuring the line intensities of the standard γ-sources of ^{241}Am ($E_\gamma = 59.6$ keV), ^{57}Co (122 and 136 keV), ^{226}Ra (186, 295, 532 and 609.4 keV), ^{137}Cs (662 keV) and ^{60}Co (1.17 and 1.33 MeV), by replacing each of them in the position of the α-particles of the ^{226}Ra source.

The measurements of the bremsstrahlung photons in coincidence with the α-particles for five α groups from the decays of ^{226}Ra ($E_\alpha = 4.784$ MeV), ^{210}Po (5.304 MeV), ^{222}Rn (5.490 MeV), ^{218}Po (6.002 MeV) and ^{214}Po (7.687 MeV) [12] were performed during about 1500 hours, and the total number of α-γ coincidences was about $4.4 \cdot 10^6$ events. For other details, see fig. 1 of our previous paper [2]. The analysis of the events reported in the (E_γ *vs.* E_α)-plane located in the region of the total energy conservation line $E_\gamma + E_\alpha = const$ (taking into account the detectors energy resolutions of 20 keV for α-particles and 32 keV for photons), gives us the possibility to determine the yield of photons at energies up to 803 keV (1st excited state of the daughter ^{206}Pb nucleus) for the α-decay of ^{210}Po. The range of (E_γ *vs.* E_α) coincidences was collected for one of the experimental run with the measurement time of about 150 hours. The $E_\gamma + E_\alpha = const$ lines for α_1(^{226}Ra), α_2(^{210}Po) and α_5(^{214}Po) groups gave the same result of the ones shown in fig. 2 of our previous paper [2].

In this last cited figure, the slope angle of the $E_\gamma + E_\alpha = const$ line was determined by using the "islands" of high-density events on the E_γ *vs.* E_α coincidence plane due to the coincidences between γ_1-lines and α-particles for the 186 keV line of ^{222}Rn and for the 510 keV line of ^{218}Po. As an example we report in fig. 1 of the present paper the TAC spectra for the "true + random" coincidences distributed along the $E_\gamma + E_\alpha = const$ line, for all events at energies $E_\gamma > 200$ keV with the α-particles emitted from ^{214}Po (full circles). For a comparison, we also report in this figure the random coincidences (open circles) when the time window of the TAC was shifted of 200 ns. In the cited figure we add the coincidences for the $E_\gamma + E_\alpha = const$ line of ^{210}Po (open stars).

There is a contribution in the peak of the TAC spectrum of the conservation line of ^{214}Po due to the coincidences between the γ_1-line (800 keV) and α-particles decaying to the first excited level of ^{210}Pb. The influence of these coincidences is observed as a small peak in the TAC spectrum of the shifted line also (due to crossing the line with the Compton distribution from the γ_1-α coincidences). Moreover, the origin of the big coincidence peak for the TAC spectrum of ^{210}Po is due to the influence of the neighboring 186, 415 and 448 keV γ-lines related to the α-decay of ^{226}Ra. After extraction of these lines from the energy spectrum of photons, "collected" along the conservation line of ^{210}Po, the transformed peak was similar to the one for the ^{214}Po nucleus.

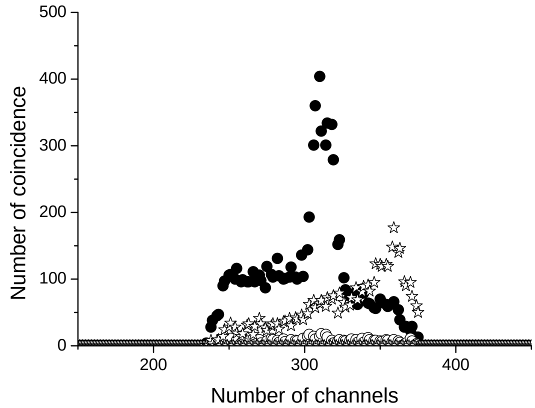

Fig. 1. The γ-α coincidences (true + random) (full circles) related to the α-decay of ^{214}Po, when the 10 ns window is set around the prompt peak of the TAC, and random ones only (open circles) when the 10 ns window was shifted by about 200 ns. In the figure we also report the real coicidences related to the α-decay of ^{210}Po (open stars).

A more detailed analysis of the recorded events was presented in [2].

To take into account the defined angular dimensions of the detectors we use the same procedure to obtain the angular averaged probability of the photon emission $\mathrm{d}P/\mathrm{d}E_\gamma$ as described in [4,5], where the α-γ angular-correlation function $W(\theta)$ for the case of the $E1$ dipole photon emission and the point-like α-γ source is

$$W(\theta) = 1 + A_2 \cdot Q_2 \cdot P_2(\cos\theta). \quad (1)$$

Here, $A_2 = -1$ for the $E1$ dipole transitions, $P_2(\cos\theta)$ is the second-order polynome of Legendre, Q_2 is the total geometrical attenuation coefficient of the second order: $Q_2 = Q_2^\alpha \cdot Q_2^\gamma$, $Q_2^{\alpha,\gamma}$ being the geometrical attenuation coefficients for the α-particle and photon detectors.

The exact calculation in the framework of the density matrix theory [13] gives us the real experimental geometry values of the attenuation coefficients: for the α detector is $Q_2^\alpha = 0.90$ and for the γ detector the value of the Q_2^γ-coefficent is varied from $Q_2^\gamma = 0.66$ for $E_\gamma = 100$ keV up to $Q_2^\gamma = 0.76$ for $E_\gamma = 800$ keV.

The probability of the photon emission at the angle θ can be written as [2,3]

$$\frac{\mathrm{d}^2 P}{\mathrm{d}E_\gamma \mathrm{d}\Omega_\gamma} = N_{\alpha\text{-}\gamma}(\theta, E_\gamma)/(\Delta T_{meas} \cdot n_\alpha \varepsilon_\gamma(E_\gamma) \cdot W(\theta)), \quad (2)$$

where $N_{\alpha\text{-}\gamma}(\theta, E_\gamma)$ is the total number of the α-γ coincidences during the measurement time ΔT_{meas} in the intervals of photon energies $E_\gamma \pm \Delta E_\gamma/2$ and angles $\Omega_\gamma \pm \Delta\Omega_\gamma/2$, n_α is the intensity of particles in the α detector, and $\varepsilon_\gamma(E_\gamma)$ is the absolute efficiency of the γ detector. Therefore, the total probability of the bremsstrahlung emission is

$$\mathrm{d}P/\mathrm{d}E_\gamma = 4\pi \cdot \mathrm{d}^2P/\mathrm{d}E_\gamma \mathrm{d}\Omega_\gamma. \quad (3)$$

The check on the experimental data has been made by measuring the coincidences between the emitted α-particles leading to the first excited level of the daughter nuclei ^{222}Rn, ^{218}Po and ^{210}Pb, and the corresponding γ-rays with energies 186, 510 and 800 keV [12].

The angular-correlation function $W(\theta)$, in the case of γ-ray $E2$ transitions, can be presented as [13]

$$W(\theta) = 1 + A_2 \cdot Q_2 \cdot P_2(\cos\theta) + A_4 \cdot Q_4 \cdot P_4(\cos\theta), \quad (4)$$

where $A_2 = 5/7$, $A_4 = -12/7$, $Q_{2,4} = Q^\alpha_{2,4} \cdot Q^\gamma_{2,4}$, $Q^\alpha_4 = 0.68$, $Q^\gamma_4 = 0.16$ for $E_\gamma = 100$ keV and $Q^\gamma_4 = 0.37$ for $E_\gamma = 800$ keV.

The obtained probabilities of the γ-transitions from the first excited state of the ^{222}Rn, ^{218}Po, ^{210}Pb nuclei are equal to $(3.4\pm0.1)\cdot10^{-2}$, $(6.3\pm0.3)\cdot10^{-4}$, $(1.1\pm0.2)\cdot10^{-4}$ 1/decay, respectively. These values are in agreement with the data of ref. [12]: $3.5\cdot10^{-2}$, $7.6\cdot10^{-4}$ and $1.4\cdot10^{-4}$ for the γ-decay of the ^{222}Rn, ^{218}Po and ^{210}Pb nuclei, respectively.

The bremsstrahlung spectra have been averaged over a photon energy interval of 25 keV.

Another test has been made by the measurements of the atomic K-shell ionization probabilities in the α-decays of ^{210}Po and ^{214}Po. The obtained values $(2.2 \pm 0.3) \cdot 10^{-6}$ and $(6.1 \pm 0.3) \cdot 10^{-6}$ 1/decay, respectively, are in agreement with our old data [14] ($(2.15 \pm 0.22) \cdot 10^{-6}$ and $(5.8 \pm 0.19) \cdot 10^{-6}$ 1/decay) and with the averaged value over various experiments for the α-decay of ^{210}Po ($(1.90 \pm 0.15) \cdot 10^{-6}$) [15].

3 Results and discussion

The new measured values of the photon emission probability $\mathrm{d}P/\mathrm{d}E_\gamma$ due to the bremsstrahlung process accompanying the α-decay of ^{214}Po are shown by full circles in fig. 2, together with our old results [2] (open circles in the present fig. 2). As one can see, our new and old experimental data have some discrepancy, which is related to the different estimations of the X- and γ-ray contributions at low (< 200 keV) and intermediate (300–500 keV) energies. In our previous paper [2] we extracted the X- and γ-ray contributions by using a line approximation of the energy dependence in the background yield at the region of the analyzed peaks, taking into account only the influence of the 186 keV line (the γ-decay of the ^{222}Rn nucleus following the α-decay of ^{226}Ra) on the low-energy part of the bremsstrahlung spectrum. In the case of the present data we extracted the peaks by using the Gaussian approximation of peaks (little increasing the uncertainty on the E_γ energy), and the cut-off of the Compton contribution for the γ-rays at high energies (strongly reducing the uncertainty on the $\mathrm{d}P/\mathrm{d}E_\gamma$ of the experimental data). In this case we also took into account the influence on the bremsstrahlung spectrum of other γ-lines up to the contribution of the 800 keV line (the γ-decay of the ^{210}Pb nucleus following the α-decay of ^{214}Po). Such a procedure also allowed us for a more detailed estimation of the uncertainties on the data for the E_γ energy and bremsstrahlung photon emission probability. Moreover, our new data of the photon emission probability $\mathrm{d}P/\mathrm{d}E_\gamma$ are extended up to 765 keV of the bremsstrahlung emission accompanying the α-decay of ^{214}Po, and this spectrum shows some slight structures.

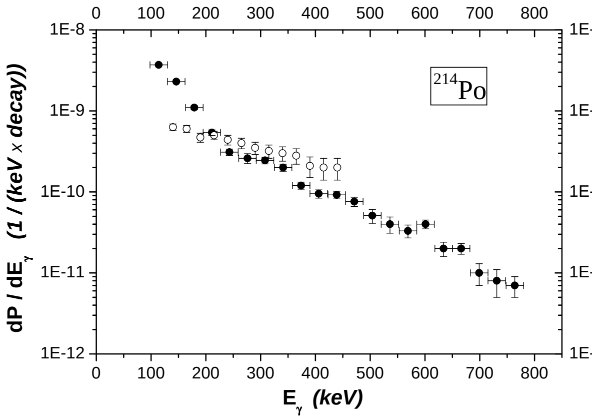

Fig. 2. The photon emission probability $\mathrm{d}P/\mathrm{d}E_\gamma$ accompanying the α-decay of ^{214}Po. Full circles are the new present experimental data, open circles are our old data of ref. [2].

In the following sect. 4 we calculate the bremsstrahlung spectrum accompanying the α-decay of ^{214}Po, and we present for a comparison the above results for ^{214}Po with the ones available in the literature [6,11] for ^{210}Po. In the theoretical description of the bremsstrahlung emission during the α-decay there are some problems: one is the choice of the realistic wave function of the α-particle inside the nuclear potential [16]. For example, the shape of the nuclear potential (the values of the nuclear radius R_n and the deepness V_n for a rectangular potential) influences the slope of the wave function near the nuclear surface and therefore the conditions of tunneling through the Coulomb barrier. Other problems are connected with the influence of the nuclear-surface deformation and electron screening on the Coulomb barrier.

4 Model, calculations and analysis

4.1 Calculation method

In our analysis we use the model developed by Maydanyuk and Olkhovsky in [17,18]. According to the calculations and analysis in [18] (see fig. 1, curves 4, 6 and 7 of the cited paper), this model and the approaches of Papenbrock and Bertsch [6], Takigawa *et al.* [7], Tkalya [8] are consistent for ^{210}Po, and such results are in a good agreement with the experimental data of Boie *et al.* [11] for this nucleus.

Let us describe the main points of our model. We define the bremsstrahlung probability during the α-decay of a nucleus in terms of the transition matrix elements for the composite quantum system (α-particle and daughter nucleus) from its state before the photon emission (we name such a state as the *initial* i*-state*) into its state after the photon emission (we name such state as the *final* f*-state*). If one considers the decaying nucleus and the process of the α-decay in the spherically symmetric approximation, then one can write the expression for the total bremsstrahlung probability with the separation of the radial and angular components explicitly by an analytical way. Here, the radius defines the position of the particle relatively to the center of mass. The angular components contain all the detailed informations about the directions of the particle motion (taking into account its tunneling) before and after the photon emission, and the one of the photon emission. This gives a more realistic estimations of the bremsstrahlung emission from the space region of the nuclear forces and the one from the tunneling region, contributing to the total bremsstrahlung spectrum. In [18] a form of the wave function (WF) of the photon emission was proposed, describing the bremsstrahlung emission during the α-decay as a function of ϑ (angle between the directions of the leaving particle and the photon). We use the expansion of the wave function of the photon (by the spherical waves [18] or in the multipolar approach [17]) without the dipole approximation and without Fermi's golden rule assumed in [6].

According to [18] we define the bremsstrahlung probability as

$$\frac{\mathrm{d}P(w,\vartheta)}{\mathrm{d}E_\gamma} = N_0 k_f w \left|p(w,\vartheta)\right|^2, \tag{5}$$

where

$$N_0 = \frac{Z_{\mathrm{eff}}^2 e^2}{(2\pi)^4 m}, \tag{6}$$

$$p(w,\vartheta) = -\sqrt{\frac{1}{3}} \sum_{l=0}^{+\infty} i^l (-1)^l \,(2l+1)\, P_l(\cos\vartheta) \cdot \sum_{\mu=-1,1} h_\mu J_{m_f}(l,w), \tag{7}$$

$$h_\pm = \mp\frac{1}{\sqrt{2}}(1\pm i), \quad k_{i,f} = \sqrt{2mE_{i,f}}, \quad w = E_i - E_f. \tag{8}$$

In (7) $J_{m_f}(l,w)$ is the radial integral independent of the angle ϑ:

$$J_{m_f}(l,w) = \int_0^{+\infty} r^2\, R_f^*(r,E_f)\, \frac{\partial R_i(r,E_i)}{\partial r}\, j_l(kr)\, \mathrm{d}r. \tag{9}$$

In the determination of WFs of the initial and final states we use the following selection rules for the quantum numbers l and m:

$$\begin{array}{l} i\text{-state before emission: } l_i = 0,\ m_i = 0; \\ f\text{-state after emission: } l_f = 1,\ m_f = -\mu = \pm 1. \end{array} \tag{10}$$

In (9) $j_l(kr)$ is the spherical Bessel function of order l, $P_l(\theta)$ is Legendre's polynomial of order l, Z_{eff} and m are the effective charge and reduced mass, respectively; $E_{i,f}$ and $k_{i,f}$ are the total energy and wave vector of the particle in the initial i-state or final f-state, respectively; $R_i(r)$ and $R_f(r)$ are the radial components of the total wave functions $\psi_i(\mathbf{r})$ and $\psi_f(\mathbf{r})$ of the system in the initial i- and final f-state, respectively; $w = k = |\mathbf{k}|$ and $\mathbf{k}$ are the energy and wave vector of the emitted photon, respectively. We use the Coulombian calibration, where the polarization vectors $\mathbf{e}^{(\alpha)}$ for each photon are perpendicular to the wave vector $\mathbf{k}$. Moreover, we use the system of units: $\hbar = 1$ and $c = 1$. Such notations are used in accordance with [17,18].

4.2 α-nucleus potential

To describe the interaction between the α-particle and the daughter nucleus we use the potentials given in [19] (see relations (6)–(10) in the cited paper, using the Coulomb $v_C(r,\theta)$, nuclear $v_N(r,\theta,Q)$ and centrifugal $v_l(r)$ components) in the general potential

$$V(r,\theta,l,Q) = v_C(r,\theta) + v_N(r,\theta,Q) + v_l(r), \tag{11}$$

where

$$v_C(r,\theta) = \frac{2Ze^2}{r}\left(1 + \frac{3R^2}{5r^2}\beta_2 Y_{20}(\theta)\right), \quad \text{for } r \ge r_m, \tag{12}$$

or

$$v_C(r,\theta) = \frac{2Ze^2}{r_m}\left\{\frac{3}{2} - \frac{r^2}{2r_m^2} + \frac{3R^2}{5r_m^2}\beta_2 Y_{20}(\theta)\left(2 - \frac{r^3}{r_m^3}\right)\right\}, \quad \text{for } r < r_m, \tag{13}$$

$$v_N(r,\theta,Q) = \frac{V(A,Z,Q)}{1 + \exp\dfrac{r - r_m(\theta)}{d}}, \tag{14}$$

$$v_l(r) = \frac{l\,(l+1)}{2mr^2}. \tag{15}$$

We define the parameters of the Coulomb and nuclear components as (see relations (14), (16)–(19) in [19])

$$V(A,Z,Q) = -(30.275 - 0.45838\, Z/A^{1/3} + 58.270\, I - 0.24244\, Q), \tag{16}$$

$$R = R_p\,(1 + 3.0909/R_p^2) + 0.1243\, t, \tag{17}$$

$$R_p = 1.24\, A^{1/3}\,(1 + 1.646/A - 0.191\, I), \tag{18}$$

$$t = I - 0.4\, A/(A+200), \tag{19}$$

$$d = 0.49290, \tag{20}$$

$$I = (A - 2Z)/A. \tag{21}$$

According to relations (21)–(22) in [19], we also use

$$r_m(\theta) = 1.5268 + R(\theta), \qquad R(\theta) = R\,(1 + \beta_2 Y_{20}(\theta)). \tag{22}$$

Here, A and Z are the nucleon and proton numbers of the daughter nucleus, respectively; Q is the Q-value for the α-decay, R is the radius of the daughter nucleus, $V(A, Z, Q, \theta)$ is the strength of the nuclear component; r_m is the effective radius of the nuclear component, d is the parameter of the diffuseness; $Y_{20}(\theta)$ is the spherical harmonic function of the second order, θ is the angle between the direction of the leaving α-particle and the axis of the axial symmetry of the daughter nucleus; β_2 is the parameter of the quadruple deformation of the daughter nucleus [20].

4.3 Spherically symmetric α-decay

According to [21], the deformation parameter β_2 for the decaying ^{214}Po nucleus is sufficiently small that allows us to apply the spherically symmetric approximation for the α-nucleus potential (11)–(22), and to use formulas (5)–(9) for the calculation of the bremsstrahlung spectrum during the α-decay of such a nucleus.

In order to obtain the spectrum, we have to know the WFs in the initial and final states. In the spherically symmetric approximation one can rewrite the total WFs by separating the radial and angular components:

$$\begin{aligned} \varphi_i(r,\theta,\phi) &= R_i(r)\, Y_{l_i m_i}(\theta,\phi) = \frac{\chi_i(r)}{r}\, Y_{l_i m_i}(\theta,\phi), \\ \varphi_f(r,\theta,\phi) &= R_f(r)\, Y_{l_f m_f}(\theta,\phi) = \frac{\chi_f(r)}{r}\, Y_{l_f m_f}(\theta,\phi). \end{aligned} \tag{23}$$

We find the radial components $\chi_{i,f}(r)$ numerically on the base of the given α-nucleus potential. Here, we use the following boundary conditions: the i-state of the system before the photon emission is a pure decaying state, and therefore for its description we use the WF for the α-decay; after the photon emission the state of the system is changed and it is more convenient to use the WF as the scattering of the α-particle by the daughter nucleus for the description of the f-state. So, we impose the following boundary conditions on the radial components $\chi_{i,f}(r)$:

$$\begin{aligned} &\text{initial } i\text{-state: } \chi_i(r \to +\infty) \to G(r) + iF(r), \\ &\text{final } f\text{-state: } \chi_f(r = 0) = 0, \end{aligned} \tag{24}$$

where F and G are the Coulomb functions as used in [18].

Let us note that the requirement of the existence of the outgoing radial flow in the asymptotic region of r (for the description of the α-decay process), constructed on the base of the radial component $\chi_i(r)$ of the initial i-state, gives a divergence (singularity) of the component $R_i(r)$ at $r = 0$ for an absolutely arbitrary shape of the potential $V(r)$ because of the conservation law of the flow inside the whole axis r. Despite such divergences, it is possible to obtain convergent values for the integrals (9) and the bremsstrahlung spectrum (5).

4.4 Bremsstrahlung spectrum for ^{214}Po

We have applied the described method to calculate the bremsstrahlung spectrum emitted during the α-decay of the ^{214}Po nucleus. The results are presented in fig. 3. Here, the angle ϑ between the directions of the α-particle motion (with possible tunneling) and the photon emission is equal to 90°. In the calculation of $p(w, \vartheta)$ in (7) we have used only $l = 0$ because the next value l does not give a noticeable deformation of the bremsstrahlung spectrum. The calculations are in rather good agreement with the experimental data and this confirms the effectiveness of our calculation method and analysis. Let us note the following:

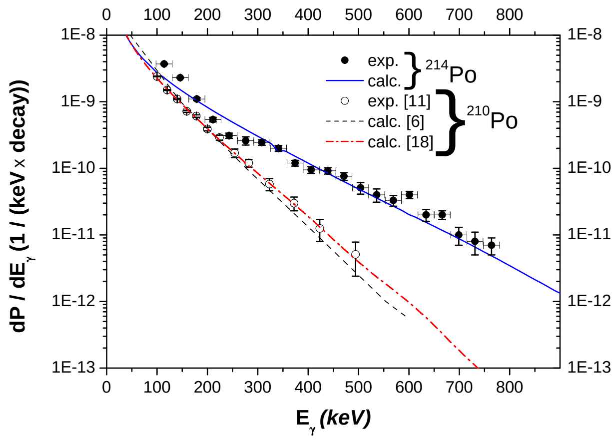

Fig. 3. Calculation (full line) of the photon emission probability $\mathrm{d}P/\mathrm{d}E_\gamma$ accompanying the α-decay of ^{214}Po (E_α = 7.7 MeV). Our new experimental data $\mathrm{d}P/\mathrm{d}E_\gamma$ for ^{214}Po (full circles), presented in fig. 2, are also reported. For a comparison, we also include the experimental data [11], the calculation [6] and the one by our approach (see line 7 of fig. 1 in [18]), obtained for the α-decay of ^{210}Po ($E_\alpha = 5.3$ MeV).

– At present, ^{214}Po is the first nucleus for which such good agreement has been achieved inside the region of the photon energy up to 750 keV (see refs. [2–5, 11]). Note that increasing the photon energy also rises the difficulty to obtain both reliable experimental data and calculation of the convergent spectra. This becomes more apparent at E_γ energies higher than about 400 keV.
– Analyzing the experimental data, one can see the presence of slight oscillations in them by comparing the experimental data with the calculated curve. One can suppose that just these oscillations can contain a new experimental information about the α-decay dynamics, because the presented calculated spectrum, obtained without taking the dynamics and deformations into account, is a monotonically decreasing function. We expect that one can obtain a more realistic dynamical description of the bremsstrahlung during the α-decay taking into account the multiple internal reflections of waves, formed in the tunnelling of the α-particle through the barrier [22]. In the same fig. 3 we also report, for a comparison, the experimental data [11] for the ^{210}Po and the related calculations obtained by Papenbrock and Bertsch [6], and by our approach [18]. As fig. 3 shows, both experimental and theoretical results of the photon emission probability obtained for the α-decay of ^{214}Po are clearly higher than the ones obtained for ^{210}Po. The difference between the two sets of data can be attributed to the

different structure of the two nuclei, which strongly affects the motion of the α-particle inside the barrier. The rate between the two sets of the photon emission probability $\mathrm{d}P/\mathrm{d}E_\gamma$ also is strongly due to the different α-decay energy for ^{214}Po ($E_\alpha = 7.7$ MeV) and ^{210}Po ($E_\alpha = 5.3$ MeV) concerning the shapes of the α-nucleus barriers for these nuclei. In fact, Papenbrock and Bertsch [6] affirm, by a simplified estimation, that the predicted rate increases with the increase of E_γ, and at $E_\gamma = 0.6$ MeV is for ^{214}Po many tens times higher than for ^{210}Po. Here, the slope angle of the bremsstrahlung spectrum can be directly connected with the relative contributions of the photon emission from tunneling and the external regions into the total spectrum. Therefore, such a slope can give new information about the value of the α-particle motion through the barrier and the α-decay half-life.

5 Conclusion

We have obtained a good agreement between theory and experiment for the bremsstrahlung spectrum of photons emitted during the α-decay of the ^{214}Po nucleus, for photon energies up to 765 keV.

In the experimental data we note the presence of slight oscillations. We think that it is possible to explain them including into the model of the dynamical description of the α-decay, deformation of the α-nucleus potential, and screening of this potential by the electrons of the atomic shells. In such a context, an interesting perspective was open by M.Y. Amusia *et al.* [23] which takes into account a new mechanism of the photon emission during the α-decay by the effect of the above-mentioned electrons.

G. Giardina is grateful to the Fondazione Bonino-Pulejo (FBP) of Messina for the important support received in the international collaboration between the Messina group and the Moscow State University (Russia) with the Institute for Nuclear Research of Kiev (Ukraine).

References

1. I.S. Batkin *et al.*, Sov. J. Nucl. Phys. **44**, 946 (1986).
2. A. D'Arrigo *et al.*, Phys. Lett. B **332**, 25 (1994).
3. N.V. Eremin *et al.*, Phys. Rev. Lett. **85**, 3061 (2000).
4. J. Kasagi *et al.*, Phys. Rev. Lett. **79**, 371 (1997).
5. J. Kasagi *et al.*, J. Phys. G. **23**, 1451 (1997).
6. T. Papenbrock, G.F. Bertsch, Phys. Rev. Lett. **80**, 4141 (1998).
7. N. Takigawa *et al.*, Phys. Rev. C **59**, 593 (1999).
8. E.V. Tkalya, Phys. Rev. C **60**, 054612 (1999).
9. M.I. Dyakonov, Phys. Rev. C **60**, 037602 (1999).
10. A. D'Arrigo *et al.*, Phys. At. Nucl. **56**, 328 (1993).
11. H. Boie, H. Scheit, U.D. Jentschura, F. Köck, M. Lauer, A.I. Milstein, I.S. Terekhov, D. Schwalm, Phys. Rev. Lett. **99**, 022505 (2007).
12. R.B. Firestone, V.S. Shirley, *Table of Isotopes*, eight edition (Lawrence Berkley National Laboratory, 1996).
13. A.J. Ferguson, *Angular correlation methods in gamma-spectroscopy*, Russian edition (Atomizdat, Moscow, 1969); D.C. Camp, A.L. Van Lehn, Nucl. Instrum. Methods **76**, 192 (1969).
14. N.V. Eremin, V.F. Strizhov, A.F. Tulinov, O.V. Ulianova, Nuovo Cimento A **97**, 629 (1987).
15. J. Law, Nucl. Phys. A **286**, 339 (1977).
16. S.D. Kurgalin, Yu M.Chuvilsky, T.A. Churakova, Izv. Akad. Nauk Ser. Fiz. **65**, 666 (2001) (in Russian).
17. S.P. Maydanyuk, V.S. Olkhovsky, Prog. Theor. Phys. **109**, 203 (2003).
18. S.P. Maydanyuk, V.S. Olkhovsky, Eur. Phys. J. A **28**, 283 (2006).
19. V. Y. Denisov, H. Ikezoe, Phys. Rev. C **72**, 064613 (2005).
20. E. Browne, Nucl. Data Sheets **65**, 209 (1992).
21. I. Muntyan, *Deformed superheavy nuclei*, PhD Thesis, University of Warsaw (2003) p. 64.
22. S.P. Maydanyuk, V.S. Olkhovsky, A.K. Zaichenko, J. Phys. Stud. **6**, 1 (2002) nucl-th/0407108; F. Cardone, S.P. Maydanyuk, R. Mignani, V.S. Olkhovsky, Found. Phys. Lett. **19**, 441 (2006).
23. M.Y. Amusia, B.A. Zon, I.Y. Kretinin, J. Exp. Theor. Phys. **105**, 343 (2007).